GRA25 Is a Novel Virulence Factor of *Toxoplasma gondii* and Influences the Host Immune Response

Anjali J. Shastri, Nicole D. Marino, Magdalena Franco, Melissa B. Lodoen,* John C. Boothroyd

Department of Microbiology and Immunology, Stanford University School of Medicine, Stanford, California, USA

The obligate intracellular parasite *Toxoplasma gondii* is able to infect a broad range of hosts and cell types due, in part, to the diverse arsenal of effectors it secretes into the host cell. Here, using genetic crosses between type II and type III *Toxoplasma* strains and quantitative trait locus (QTL) mapping of the changes they induce in macrophage gene expression, we identify a novel dense granule protein, GRA25. Encoded on chromosome IX, GRA25 is a phosphoprotein that is secreted outside the parasites and is found within the parasitophorous vacuole. *In vitro* experiments with a type II Δ*gra25* strain showed that macrophages infected with this strain secrete lower levels of CCL2 and CXCL1 than those infected with the wild-type or complemented control parasites. *In vivo* experiments showed that mice infected with a type II Δ*gra25* strain are able to survive an otherwise lethal dose of *Toxoplasma* tachyzoites and that complementation of the mutant with an ectopic copy of *GRA25* largely rescues this phenotype. Interestingly, the type II and type III versions of GRA25 differ in endogenous expression levels; however, both are able to promote parasite expansion *in vivo* when expressed in a type II Δ*gra25* strain. These data establish GRA25 as a novel virulence factor and immune modulator.

*T*oxoplasma gondii is an obligate intracellular parasite with the remarkable ability to infect a broad range of mammalian and avian hosts. During infection in the mouse, a natural *Toxoplasma* host, macrophages are known to play a key role in mounting an immune response to infection via the secretion of cytokines such as interleukin-12 (IL-12) and tumor necrosis factor alpha (TNF-α) (1). The secretion of these cytokines leads to the activation of NK cells and CD4$^+$ and CD8$^+$ T cells (2–4). Although macrophages can themselves be targets of parasite infection, they also can control parasite dissemination through cell-intrinsic, antimicrobial strategies, such as the production of nitric oxide (NO) and reactive oxygen species (ROS) and, in mice, the activation of immunity-related GTPases (IRGs) (5, 6). Recent studies have shown that inflammatory monocytes, in particular, are recruited to the site of infection by the cytokine CCL2 (monocyte chemotactic protein-1 [MCP-1]) (7, 8). As has been described for infection with several pathogens (9), CCL2 is essential for control of parasite spread and survival of infection in both intraperitoneal (i.p.) and oral *Toxoplasma* infections (7, 8).

The strains of *Toxoplasma* that predominate in Europe and North America, termed types I, II, and III, differ in a wide range of phenotypes, including how they interface with the immune response. The tachyzoite stage of the parasite interacts with the host through secretion of polymorphic proteins from specialized organelles termed rhoptries, which house "ROP" proteins, and dense granules, which contain "GRA" proteins. One such polymorphic protein is the tyrosine kinase ROP16. Upon injection into the host cell, it directly phosphorylates STAT3 and STAT6, and in cells infected with types I and III, but not in type II-infected cells, this effect is sustained (10–12). Another strain-specific effector, GRA15, mediates NF-κB nuclear activation and NF-κB-mediated transcription in cells infected with type II but not type I or III parasites (13). These proteins drastically alter host cell gene expression and contribute to strain-specific differences in macrophage polarization and inflammation in the intestines of infected mice *in vivo* (14). Other polymorphic effectors that target macrophage antimicrobial pathways include the pseudokinase ROP5

and kinase ROP18, which together inactivate host IRGs, preventing degradation of the parasitophorous vacuole (PV) (15–17).

Most of the effectors described above were identified through analysis of genetic crosses between *Toxoplasma* types to identify the parasite factors that mediate strain-specific phenotypes. For example, ROP16 was found through quantitative trait locus (QTL) mapping of changes in host gene expression induced in infected human fibroblasts (11). As the interactions between an invading parasite and its host cell likely differ in different cell types and different host species, we hypothesized that analysis of gene expression in macrophages from the mouse, a host that has a long evolutionary history with *Toxoplasma* and a cell type that is crucial for innate immunity, would reveal previously unidentified parasite effectors that specifically modulate these key initiators of the immune response. Indeed, studies in mouse macrophages have shown that the known *Toxoplasma* effectors account for only about 40% of the strain-specific differences in gene expression observed when macrophages are infected with type II versus type III parasites (18). To identify previously unknown effectors, therefore, we have used type II versus type III F1 progeny to map parasite loci responsible for changes in mouse macrophage gene expression induced upon infection. This has led to the identification of a novel dense

granule protein, GRA25, which plays a key role in the immune response to *Toxoplasma* tachyzoites and is crucial for virulence.

MATERIALS AND METHODS

Cell culture. *Toxoplasma gondii* tachyzoites were maintained by passage in confluent primary human foreskin fibroblast (HFF) monolayers in Dulbecco modified Eagle medium (DMEM) (Invitrogen, Carlsbad, CA) with 10% fetal bovine serum (FBS; HyClone, Logan, UT), 2 mM glutamine, 100 U/ml penicillin, and 100 µg/ml streptomycin (complete DMEM [cDMEM]) at 37°C with 5% CO_2.

Mouse bone marrow-derived macrophages (mBMDMs) were derived from the femurs and tibias of female C57BL/6 mice via culture for 6 days in cDMEM–20% (final concentration) murine macrophage colony-stimulating factor (M-CSF)-containing conditioned media. RAW264.7 cells (purchased from ATCC) were grown in cDMEM supplemented with 10 mM HEPES and 1 mM sodium pyruvate.

Microarray analysis. RAW 264.7 (ATCC) cells were plated in 6-well plates. When confluent, cells were infected with one of 32 strains of *Toxoplasma* F1 progeny that were derived from crosses between type II (ME49) and type III (CEP) parasites at a multiplicity of infection (MOI) of 3 ([19], [20]). About 24 h postinfection (hpi), RNA was isolated using TRIzol reagent (Invitrogen) followed by ethanol precipitation according to the manufacturer's protocol. RNA was labeled using the One Cycle or 3′ IVT Express reaction, and labeled, fragmented cRNA was hybridized to a mouse Affymetrix array (Mouse 430 2.0) according to the manufacturer's protocol. Probe intensities were measured and processed into image analysis (.CEL) files by the PAN Facility at Stanford University. Intensity values were normalized using the Robust Multi-array Average (RMA) algorithm.

For Ingenuity pathway analysis (IPA; Qiagen, Redwood City, CA), we generated a gene list containing genes that met the criteria stated in the text (for the given experiment). A data set containing the gene identifiers for these genes (focus genes) was uploaded, and each gene identifier was mapped to its corresponding gene in the Ingenuity Pathways Knowledge Base. Canonical pathway analysis identified the pathways from the Ingenuity Pathways Analysis library that were most significant to the data set. Focus genes were also overlaid onto a global molecular network developed from information contained in the Ingenuity Pathways Knowledge Base. Networks of these focus genes were then algorithmically generated based on their connectivity.

Gene set enrichment analysis (GSEA) was used to find candidate transcription factors and canonical pathways that are modulated differently between *Toxoplasma* infections. This program uses a predefined sets of genes and determines whether the members of these sets of genes are randomly distributed throughout a ranked list or primarily found at the top or bottom of that list. As we used GSEA to generate hypotheses, gene sets enriched with a false discovery rate (FDR) < 25% were considered significant. Both transcription factor and canonical pathway gene sets from the Molecular Signatures Database were evaluated for enrichment (c3.tft.v3.symbols.gmt; c2.cp.v3.symbols). To look for enrichment of transcription factor binding sites (TFBSs) in a defined set of genes, we also used distant regulatory elements (DiRE) of coregulated genes (dire.dcode.org).

Generation of ME49Δ*gra25* and ME49Δ*gra25*:*GRA25* parasites. To create the ME49Δ*gra25* parasites, we started with a parental type II ME49-*luc*Δ*hxgprt* (ME49) strain that expresses firefly luciferase but lacks the hypoxanthine-xanthine-guanine phosphoribosyl transferase (HXGPRT) gene ([21]). The TGME49_290700 (GRA25) gene was deleted from ME49 and replaced with *HXGPRT* by homologous recombination using the pTKO2 vector ([21]) in which the *HXGPRT* is flanked by ~1 kb and ~1.5 kb, respectively, of genomic sequence amplified by PCR from the 5′ and 3′ regions flanking the TGME49_290700 open reading frame (ORF). The 5′-flanking region was amplified using 5′-GCGCGGTACCGACCTAGA GAGCATTCAACGC-3′ (forward) and 5′-GCGCGAATTCGATAACCG ACGAAGACCAGGAGAG-3′ (reverse) primer sequences and was cloned into the KpnI and EcoRI restriction sites of pTKO2 ([21]). The 3′-flanking

region was amplified using 5′-GGGGAAGCTTGAAAACGGTGCGCGG AAGG-3′ (forward) and 5′-GCGCGCTAGCCAGATTCCCCAGACGGA TTTG-3′ (reverse) primer sequences and was cloned into HindIII and NheI restriction sites of the pTKO2 vector. The resulting pGRA25_KO vector was linearized with HpaI, and 30 µg of the linearized plasmid was transfected into ME49-*luc*Δ*hxgprt* parasites by electroporation, as previously described ([22]). The parasites were allowed to infect HFFs in 24-well plates for 24 h, after which the medium was changed to cDMEM supplemented with 50 µg/ml mycophenolic acid (MPA) and 50 µg/ml xanthine for HXGPRT selection. The parasites were passed twice into 24-well plates before being cloned using a single-cell method into 96-well plates. The Δ*gra25* and control clones were identified by PCR of the open reading frame using the 5′-GCGCACAACCGTGACTTCCACGA-3′ (forward) and 5′GCGCATGTGGACACAGTCGGTTGA-3′ (reverse) primer sequences. Integration at the 3′ end was confirmed by PCR with the following primers: 5′-GCGCCAACTCCTCGCCGAAGTAAG-3′ (forward) and 5′-GCGCAACACAAGAACCCGTTGAGG-3′ (reverse).

To transfer (complement) the GRA25 locus back into the knockout (KO) strain, the *HXGPRT* marker was first removed using Cre recombinase as previously described ([21]). Briefly, a plasmid expressing Cre recombinase was transiently transfected into the ME49Δ*gra25* strain to catalyze recombination at the *loxP* sites flanking the HXGPRT marker in the pGRA25_KO vector. After growth in 350 µg/ml 6-thioxanthine to select for loss of HXGPRT, single clones were isolated via limiting dilution. These clones were confirmed to be sensitive to MPA-xanthine due to the removal of the *HXGPRT* gene. Single ME49Δ*gra25*Δ*hxgprt* clones were used to generate ME49Δ*gra25*:*GRA25*-complemented strains. To do this, Δ*gra25*Δ*hxgprt* parasites were transfected by electroporation with the pGRA25_II_HA vector, which represents the pGRA-HA_HXGPRT vector ([23]) modified to contain the coding region of type II GRA25 (from ME49) plus ~1.2 kb 5′ of the start codon. The GRA25_II open reading frame (minus the stop codon) was amplified from ME49 genomic DNA using the following primers: 5′-GC GC ATG CAT ATG AAG CGT TTC TGG TTG TGC G-3′ (forward) and 5′-GCGC ACATGT GTT TCT ATC GAA TTC CGG GAG-3′ (reverse). The resulting ~1-kb fragment was digested with NsiI and PciI restriction enzymes and cloned into the NsiI and NcoI restriction sites of the pGRA-HA_HPT vector to create pGRA_GRA25_II_HA. Next, we removed the GRA1 promoter from pGRA_GRA25_II_HA vector through digestion of the vector with HindIII and NsiI. From ME49 genomic DNA, ~1.2 kb 5′ of the start codon of *GRA25* was amplified using the following primers: 5′-GC GC AAGCTT CTA AAC TAC TCA CAT CAT AGG-3′ (forward) and 5′-GC ATGCAT TGT GCT CCG GCC TCG CGC GCA TT-3′ (reverse). The resulting ~1.2-kb fragment, which is presumed to include the bulk of the GRA25 promoter, was digested with HindIII and NsiI and cloned into the pGRA_GRA25_II_HA vector digested as described above to create the pGRA25_II_HA vector. After transfection of 15 µg of this vector in Δ*gra25*Δ*hxgprt* parasites, integration was selected for using MPA-xanthine as described above and subjected to a single-cell cloning procedure using limiting dilution. Expression of GRA25_II was determined by Western blot and immunofluorescence analyses using anti-hemagglutinin (anti-HA) antibodies and anti-GRA25 antisera.

To complement the *gra25*-deficient parasites with the type III allele of GRA25, ME49Δ*gra25*Δ*hxgprt* parasites were transfected by electroporation with the pGRA25_III_HA vector, which represents the pGRA-HA_HXGPRT vector ([23]) modified to contain the coding region of GRA25 from type III (CEP) parasites plus ~1.2 kb 5′ of the start codon, including its presumptive promoter. To generate the pGRA25_III_HA vector, we amplified the relevant genomic regions using primers 5′-GCGC AAG CTT CTAAACTATTCACATCATAGGCTCCTG-3′ (forward) and 5′-GC GC ACA TGT GTT TCT GTC GAA TTC CGG GAG-3′ (reverse). The resulting ~2-kb fragment was digested with HindIII and PciI restriction enzymes and cloned into the HindIII and NcoI restriction sites of the pGRA-HA_HXGPRT vector, thereby also removing the GRA1 promoter

and yielding a plasmid exactly analogous to the pGRA25$_{II}$_HA vector. The resulting vector was linearized with NotI, and 15 μg of this vector was used to transfect ME49 Δ*gra25*Δ*hxgprt* parasites. Integration was selected for using MPA-xanthine as described above and subjected to a single-cell cloning procedure using limiting dilution. Expression of GRA25$_{III}$ was determined by Western blot and immunofluorescence analysis (IFA) using anti-hemagglutinin (anti-HA) antibodies and anti-GRA25 antisera.

Generation of RH-expressing HA-tagged versions of GRA25. RH parasites expressing a C-terminally HA-tagged allele of GRA25 were generated by first amplifying the GRA25 open reading frame (minus the stop codon) from RH genomic DNA using the following primers: 5′-GC GC ATG CAT ATG AAG CGT TTC TGG TTG TGC G-3′ (forward) and 5′-GC GC ACA TGT GTT TCT GTC GAA TTC CGG GAG-3′ (reverse). The resulting ∼1-kb fragment was digested with NsiI and PciI restriction enzymes and cloned into the NsiI and NcoI restriction sites of the pGRA vector. The resulting vector (pGRA_GRA25$_I$_HA) was linearized with NotI, and 30 μg of the linearized plasmid was transfected into RHΔ*hxgprt* by electroporation as described above. The parasites were allowed to infect HFFs in a T25 flask for 24 h, after which the medium was changed to cDMEM supplemented with 50 μg/ml MPA and 50 μg/ml xanthine for *HXGPRT* selection. The parasites were subjected to multiple passages in T25 flasks before being singly cloned into a 96-well plate. Single clones that expressed the construct were identified by immunofluorescence using anti-HA antibodies to detect expression of the transgene.

RH parasites in which the *GRA25* gene has been endogenously tagged with a C-terminal HA tag were created using a method similar to that described above. Here, however, RHΔ*hxgprt*Δ*ku80* parasites (instead of the RHΔ*hxgprt* parasites described above) were used to minimize nonhomologous recombination. We linearized the pGRA_GRA25$_I$_HA vector with NsiI (instead of NotI as described above) so as to generate a linearized fragment beginning with the ORF of the gene. RHΔ*hxgprt*Δ*ku80* parasites were transfected with 30 μg of linearized plasmid by electroporation. The parasites were allowed to infect HFFs in a T25 flask for 24 h, after which the medium was changed to cDMEM supplemented with 50 μg/ml MPA and 50 μg/ml xanthine for HXGPRT selection. The parasites that had integrated the HA tag into the endogenous GRA25 locus were identified by IFA using anti-HA antibodies.

Generation of polyclonal antibodies. N-terminal glutathione *S*-transferase (GST)-tagged proteins were expressed using pGEX-6P1 plasmid (Agilent Technologies). GST-tagged GRA25 was generated using primers to amplify the full-length sequences from type II (ME49) parasites, excluding the predicted signal peptide. The resulting fusion protein was purified from *Escherichia coli* (Rosetta strain; Novagen/EMD Millipore) essentially as described previously (24) and injected intraperitoneally (i.p.) into female BALB/c mice with 100 μl of Ribi conjugate (Corixa, Hamilton, MT) in a total volume of 200 μl. Blood of naive female BALB/c mice was drawn prior to injection and tested against monolayers of *Toxoplasma*-infected cells and *Toxoplasma* lysate to ascertain that the sera contained no baseline reactivity to GRA25. The initial dose was 100 μg protein per mouse, followed by 50 to 75 μg protein/mouse on days 20, 40, and 63 after the initial injection. Serum was isolated on days 28, 40, and 80 after the initial injection. The presence of antibodies to the recombinant protein was assessed by IFA and Western blot analysis. All animal experiments were conducted with the approval and oversight of the Institutional Animal Care and Use Committee at Stanford University.

Immunofluorescence assays. *Toxoplasma*-infected HFF cells on glass coverslips were fixed with 2.5% to 4% formaldehyde for 20 min. All subsequent incubations were performed in phosphate-buffered saline (PBS) supplemented with 3% bovine serum albumin (BSA). The cells were permeabilized for 15 min with PBS supplemented with 0.2% Triton X-100 and subsequently were blocked in 3% BSA–PBS overnight at 4°C or at room temperature for 1 h. After incubation with the primary antibody, Alexa Fluor 594- and Alexa Fluor 488-conjugated secondary antibodies (Molecular Probes/Invitrogen) were used (25). Samples were viewed on an Olympus BX60 upright fluorescence microscope with a 100× oil im-

mersion lens, and images were acquired with Image-Pro Plus software or QCapture software (version 2.9.11.2). Rabbit antibodies to dense granule protein 7 (GRA7) were used as a control for dense granule localization (25). Polyclonal antisera to GRA25 (described above) and rat antibody to the HA tag were also used in immunofluorescence studies.

Western blots. Lysates were prepared by harvesting and lysing infected cells in Laemmli sample buffer supplemented with 14.3 M β-mercaptoethanol and 1 M dithiothreitol (DTT). Samples were boiled for 10 min, mixed using a vortex device, separated by SDS-PAGE, and transferred to a polyvinylidene difluoride (PVDF) membrane. GRA25 was detected either by the use of polyclonal antisera to GRA25 (as described above) followed by incubation with horseradish peroxidase (HRP)-conjugated goat anti-mouse IgG or by the use of monoclonal antibody 3F10 (rat anti-HA antibody) conjugated to HRP (Roche, South San Francisco, CA). Rabbit anti-SAG1 antibodies followed by anti-rabbit antibodies conjugated to HRP were used to control for parasite number. Antibody incubations were performed in Tris-buffered saline (TBS) with 5% milk and 0.1% Tween 20. Levels of HRP were detected using an ECL chemiluminescence kit (purchased from Pierce).

CIP treatment. RH parasites expressing a C-terminally HA-tagged allele of GRA25 were allowed to produce full vacuoles in HFF cells, medium was aspirated, and cells were washed 2 times with prewarmed PBS. Cells were then lysed directly into 100 μl of 2× Laemmli sample buffer. A 15-μl volume of sample was treated with either 3 μl of calf intestinal phosphatase (CIP) or PBS. A 10-μl volume of each resulting sample was then mixed with 10 μl of sample buffer and separated by SDS-PAGE. Samples were transferred to a PVDF membrane and detected by the use of monoclonal antibody 3F10 (rat anti-HA antibody) conjugated to HRP.

Cytokine secretion assays. For cytokine secretion measurements, mBMDMs were infected with *Toxoplasma* tachyzoites at an MOI of 3. At 12 hpi, supernatants were harvested and lysed using a syringe followed by passage through a 0.2-μm-pore-size filter. Filtered supernatant samples were analyzed in the Human Immune Monitoring Core (Stanford, CA) by the use of Luminex Mouse 26plex kits purchased from Affymetrix and used according to the manufacturer's recommendations with modifications as described below. Briefly, samples were mixed with antibody-linked polystyrene beads on 96-well filter-bottom plates and incubated at room temperature for 2 h followed by overnight incubation at 4°C. Plates were vacuum filtered and washed twice with wash buffer and then incubated with biotinylated detection antibody for 2 h at room temperature. Samples were then filtered and washed twice as described above and resuspended in streptavidin-phycoerythrin (PE). After incubation for 40 min at room temperature, two additional vacuum washes were performed, and the samples were resuspended in Reading Buffer. Each sample was measured in duplicate. Plates were read using a Luminex 200 instrument with a lower limit of 100 beads per sample per cytokine. Cytokines assessed by Luminex were as follows: IL-1α, IL-1β, IL-2, IL-3, CXCL10, IL-4, IL-5, IL-6, IL-10, transforming growth factor β (TGF-β), IL-12p40, IL-12p70, IL-13, gamma interferon (IFN-γ), granulocyte-macrophage colony-stimulating factor (GM-CSF), TNF-α, granulocyte colony-stimulating factor (G-CSF), MCP-3 (CCL7), eotaxin, vascular endothelial growth factor (VEGF), KC (CXCL1), IL-17, IL-23, CCL5, macrophage inflammatory protein 1 alpha (MIP-1α), and MCP-1 (CCL2).

Mouse infection. Female CBA/J mice (8 to 10 weeks old) were infected intraperitoneally with 500 tachyzoites in 200 μl PBS. The mice were housed under standard conditions and monitored daily for body weight and general signs of acute illness. Moribund animals whose body weight fell below 75% of their starting weight were euthanized.

Bioluminescence imaging. For bioluminescence imaging, mice were injected i.p. with 200 μl of D-luciferin–PBS (150 mg substrate/kg body weight), anesthetized with isoflurane, and imaged using a Xenogen IVIS-100 imaging system. Mice were imaged ventrally for 5 min. Luminescence was quantified (in photons) for the abdominal region for each mouse via the use of Living Image software.
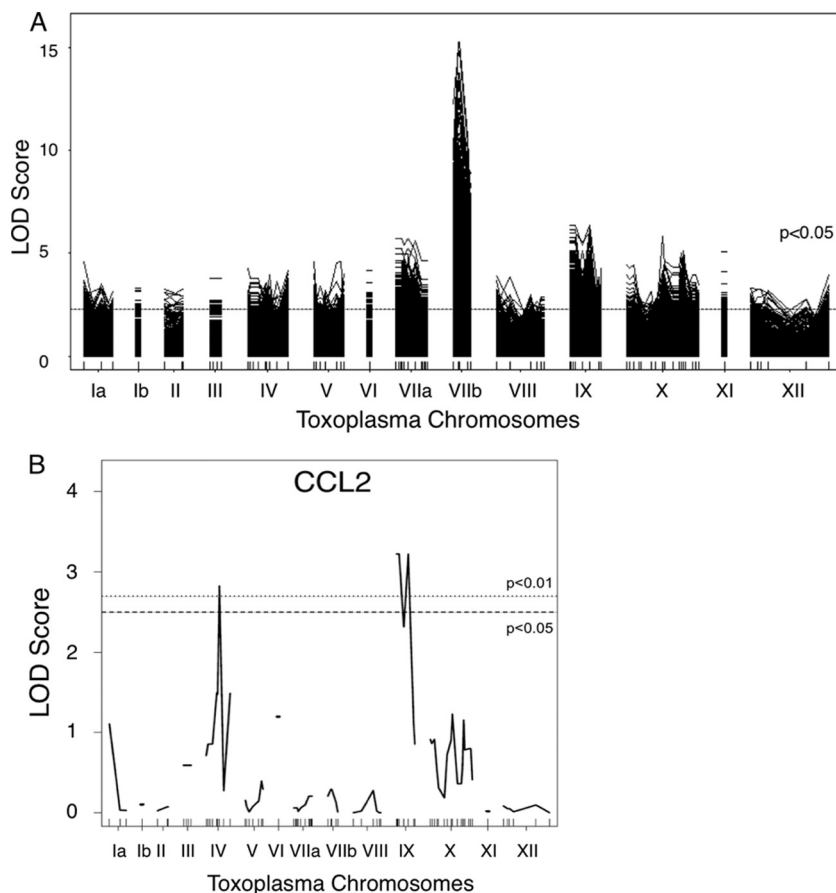
FIG 1 QTL mapping reveals several loci on *Toxoplasma* chromosomes that control the expression of mouse genes in macrophages. (A) LOD scores indicating the log likelihood of association with mouse gene expression are plotted relative to mapped markers across the *Toxoplasma* genome in numerical chromosome order. The dashed line represents the average cutoff for significance ($P < 0.05$, permutation test) across all mapped genes (LOD score = 2.3). Each solid line represents a mouse gene that maps to a genetic marker with a LOD score above the $P < 0.05$ threshold (on average, a LOD score > 2.3). (B) As in panel A, but LOD score plots are shown only for mouse CCL2 (MCP-1). The dashed line indicates a $P < 0.05$ significance threshold; the dotted line indicates a $P < 0.01$ significance threshold.

Plaque assays. Confluent HFF monolayers were infected with 500 parasites. Flasks were placed in the incubator and left untouched. At 10 days postinfection (dpi), monolayers were washed with PBS and fixed with methanol. Monolayers were then stained with crystal violet, and plaques were enumerated. Plaque areas were quantified via ImageJ.

Microarray data accession number. The entire MIAME database-compliant dataset from these experiments can be found under the NCBI Gene Expression Omnibus (GEO) accession number GSE56534.

RESULTS

QTL mapping reveals a region on *Toxoplasma* chromosome IX that controls the expression of mouse genes in macrophages. To identify novel parasite effectors that modulate the immune response to *Toxoplasma* infection, we exploited the natural variation between type II and type III strains of *Toxoplasma* with respect to their ability to interact with macrophages. We infected RAW 264.7 cells with each of 32 strains of *Toxoplasma* F1 progeny that were derived from crosses between type II and type III parasites (19, 20). At 24 h postinfection (hpi), RNA was isolated from the infected cells and analyzed by hybridization to Affymetrix Mouse 430 2.0 microarrays. The relative abundance of each host gene's mRNA was assessed, and, based on the known genetic maps for each of the progeny, *Toxoplasma* quantitative trait loci (QTL) that

associated with the differences in gene expression in infected macrophages were identified. This analysis identified >2,500 mouse genes whose expression mapped significantly to one or more *Toxoplasma* loci (Fig. 1A; see also Dataset S1 in the supplemental material). As expected, many of these mouse genes mapped to loci that encode *Toxoplasma* effectors known to mediate changes in host cell gene expression. These include chromosome VIIb (1,022 mouse genes), on which ROP16, the tyrosine kinase that activates STAT3 and STAT6, is located (10–12), and chromosome X (261 mouse genes), on which the NF-κB regulator GRA15 is located (13). As was found in previous QTL mapping analyses of human and chicken fibroblasts infected with the same *Toxoplasma* progeny (11, 26), the host genes with the highest logarithm of odds (LOD) scores, measuring the strength of the association between a *Toxoplasma* marker and host cell gene expression, mapped to chromosome VIIb (maximum LOD score = 15.22). Gene Set Enrichment Analysis (GSEA) (27) and distal regulatory element enrichment (DiRE) analysis (http://dire.dcode.org/) of the mouse genes that mapped to *Toxoplasma* chromosome VIIb indicated that their transcription was largely controlled by transcription factors STAT3, STAT5, and STAT6, which are targets of ROP16. These results indicate that ROP16 likely plays an important role in

mediating strain-specific differences in macrophage gene expression as it does in fibroblasts, a finding that has been experimentally validated in macrophage studies using ROP16-deficient parasites (14, 18, 28).

As we were interested in identifying novel parasite effectors that control host responses, we focused our attention on *Toxoplasma* chromosomes where modulators of host transcription had not previously been identified. Interestingly, expression differences in ~20% of the mouse genes mapped to *Toxoplasma* chromosome IX (492 genes), a chromosome that contains no previously described *Toxoplasma* effectors (Fig. 1A). We performed GSEA and DiRE analysis of the host genes whose expression levels mapped to chromosome IX and found that, unlike for chromosome VIIb, there was no common host transcription factor identified as regulating a majority of these genes. This suggests that there may be more than one *Toxoplasma* effector carried on chromosome IX and/or that a single effector influences host gene expression through two or more mechanisms.

Of the host genes that mapped to chromosome IX, several were immunity-related genes, including CCL2 (also known as MCP-1 [monocyte chemotactic protein-1]) (LOD score = 3.22) (Fig. 1B). CCL2 is a cytokine that is well established to be abundantly secreted during *Toxoplasma* infection (8, 29–32), and its levels of mRNA expression differ ~2.3-fold between type II-infected and type III-infected macrophages (18). CCL2 mRNA expression levels have also recently been shown to differ ~2.7-fold in peritoneal exudate cells from mice infected with type II versus type III parasites (33). Interestingly, in addition to the peak on chromosome IX, there was also a peak on chromosome IV that associated with CCL2 expression (Fig. 1B). This result suggests that, in addition to a gene on chromosome IX, there may be a locus on chromosome IV encoding another *Toxoplasma* protein that regulates expression of CCL2 in macrophages.

GRA25 is a dense granule protein on chromosome IX that is secreted outside the parasite and is phosphorylated in infected cells. To identify the immune regulator on chromosome IX, we focused on the region to which differences in CCL2 expression and expression of several other immune genes identified in Dataset S1 in the supplemental material mapped. Within this region, we used the following criteria to create a preliminary list of candidate genes based on the predicted properties of the proteins they encode: (i) a signal peptide to drive secretion of the protein outside the parasite; (ii) expressed sequence tag (EST) data and microarray data as evidence that the gene is expressed in tachyzoites; and (iii) mass spectrometry evidence confirming expression of the protein. The data described above were obtained from data sets deposited by our laboratory and by others within ToxoDB (v 7.3; www.toxodb.org). This initial list of genes was then further prioritized based on whether they were polymorphic between the strains and whether their levels of expression in tachyzoites differed across the strains, both being possible reasons for the strain-dependent differences observed in host gene expression mapping to this region. The genes of greatest interest were those with an above-average frequency of single nucleotide polymorphisms (SNPs) or a large difference between type II and type III in mRNA expression levels. This led us to focus on TGME49_290700, a gene that is abundantly expressed in tachyzoites and that has the highest coding sequence SNP density (35 SNPs in 948 nucleotides) of all the expressed genes encoding a protein with a predicted signal peptide in the relevant region of chromosome IX. This gene's pre-

dicted product has no homology to any protein outside the *Eucoccidia* (data not shown) and after removal of the signal peptide would have a predicted mass of ~32 kDa (absent any posttranslational modifications; Fig. 2A). There did not appear to be reproducible differences between the two strains in the levels of mRNA expression of this gene as reported in ToxoDB (34) or among the F1 progeny from the type II × III cross (data not shown).

To localize the 290700 protein and confirm its expression, we added a short sequence encoding an HA tag to the endogenous gene in the type I RH strain. (Type I parasites were used for these initial tests because of the ease of their genetic manipulation). Using antibodies to the HA tag, we found that, as predicted, the product of this gene is indeed secreted outside the parasite (Fig. 2B). 290700 was also reported to be phosphorylated after invasion based on phosphoproteomics data (35). To confirm the latter result, we performed gel electrophoresis on lysates of intact HFF cells infected with parasites expressing an HA-tagged version of the protein, with and without treatment with phosphatase (Fig. 2C). Consistent with the published phosphoproteomics data, we observed a slower-migrating, phosphatase-sensitive band in these "intracellular" lysates, indicating that this protein is indeed phosphorylated. The dephosphorylated version of the protein migrates as if it were ~46 kDa, suggesting that the protein is posttranslationally modified in other ways and/or migrates more slowly than predicted due to its amino acid composition (e.g., it has a stretch of 11 consecutive threonine residues).

To confirm the localization data obtained with the tagged construct in type I parasites and to extend the results to type II, we generated antibodies against recombinant TGME49_290700 as described in Materials and Methods. Immunofluorescence experiments performed on extracellular type II (ME49) parasites indicated that the native protein is abundantly present within the parasitophorous vacuole and colocalizes with dense granule protein 7 (GRA7) inside the parasites (Fig. 2D). Colocalization between TGME49_290700 and GRA7 was also seen in intracellular parasites (data not shown). Together, these data indicate that TGME49_290700, referred to here as "GRA25," is a novel phosphoprotein that is secreted from dense granules into the parasitophorous vacuole.

Generation and complementation of parasites deficient in GRA25. As demonstrated above, GRA25 has many of the attributes of a secreted *Toxoplasma* effector. To further investigate the function of this protein, we generated parasites deficient in GRA25. For these experiments, we used type II ME49 parasites, as this strain elicits a more potent immune response and induces higher levels of proinflammatory cytokines, including CCL2, than type I and type III strains (36). Type II is also the better-studied strain in the mouse model, with moderate virulence compared to type I.

The *GRA25* (TGME49_290700) gene was deleted via homologous recombination and insertion of the *HXGPRT* selectable marker (Fig. 3A). The absence of the gene was confirmed by PCR (Fig. 3B and C). To generate *GRA25*-complemented strains in the ME49Δ*gra25* background, the *HXGPRT* selectable marker, which is flanked by *loxP* sites, was first removed by transiently transfecting parasites with a CRE recombinase-expressing plasmid and selecting for loss of *HXGPRT* using 6-thioxanthine as described previously (21). Single clones of the resulting ME49Δ*gra25* strain were then transfected with the $GRA25_{II}$ gene (also from type II ME49, as indicated by the subscript "II") driven by its own pro-
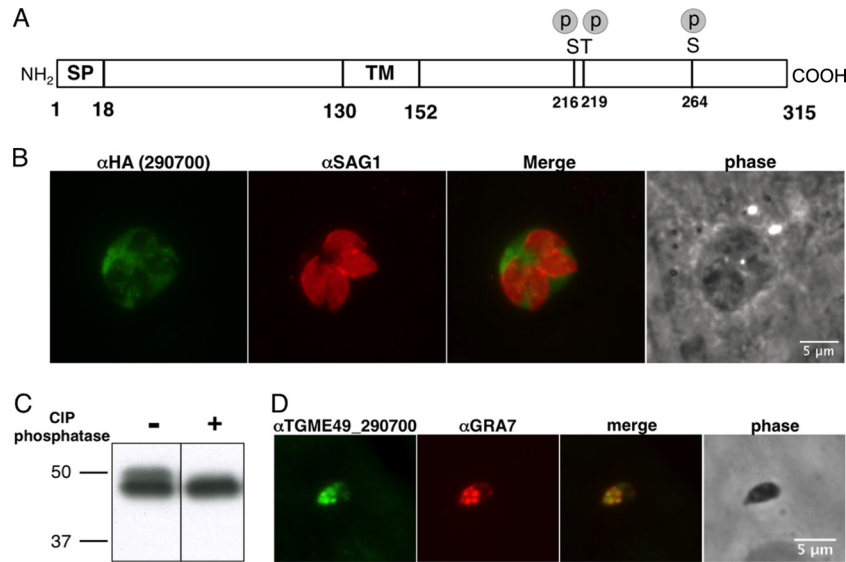
FIG 2 TGME49_290700 is a novel dense granule protein (GRA25) that is secreted into the PVM and is phosphorylated. (A) Schematic diagram of the TGME49_290700 protein. The signal peptide (SP) is as predicted by the SignalP 4.1 Server, and phosphorylated serine (S) and threonine (T) residues (p) were determined by mass spectrometry, as previously reported (17). The protein contains a hydrophobic region, predicted to be a transmembrane (TM) domain. Numbers indicate predicted amino acid positions. (B) HFF monolayers were infected with *Toxoplasma* RH parasites in which the 290700 gene has been endogenously tagged with a C-terminal HA tag. At 24 hpi, the cells were fixed, permeabilized, and visualized by immunofluorescence microscopy using antibodies to the HA tag (green) or SAG1, the tachyzoite surface antigen (parasites; red). (C) Lysates from HFFs infected with RH parasites expressing a C-terminally HA-tagged allele of 290700 were treated with or without calf intestinal phosphatase and loaded in each lane. The membrane was probed with an anti-HA antibody conjugated to peroxidase. The migration of the 50-kDa and 37-kDa size markers is shown. (D) Syringe-lysed (extracellular) type II parasites were plated on an HFF monolayer for 15 min. Samples were fixed, permeabilized, and stained using polyclonal antisera raised against TGME49_290700 recombinant protein or GRA7 as a positive control for dense granules. Samples were visualized by immunofluorescence microscopy.

moter. Western blot analysis confirmed that the GRA25$_{II}$ protein was indeed absent in the Me49Δ*gra25* parasites and was successfully reintroduced in complemented parasites (Fig. 3D). Plaquing experiments and serial passage revealed no difference between the growth of the ME49 strain and the growth of the ME49Δ*gra25* strain in human foreskin fibroblasts *in vitro* (data not shown). Additionally, infection of bone marrow-derived macrophages (BMDMs) with GRA25-deficient and GRA25-intact (wild-type [WT] or complemented) parasites revealed that there was no difference in either infectivity or parasite growth in macrophages *in vitro* (see Fig. S1 in the supplemental material). In subsequent experiments to determine the function of GRA25, the parental (ME49), KO (ME49Δ*gra25*), and complemented (ME49Δ*gra25*: GRA25$_{II}$) strains were used.

GRA25 impacts cytokine secretion and is a novel parasite virulence factor. To determine whether GRA25 influences the expression of cytokines such as CCL2, mouse bone-marrow-derived macrophages (BMDMs) were infected with ME49, ME49Δ*gra25*, or ME49Δ*gra25*:GRA25$_{II}$ parasites at an MOI of 3, and cell culture supernatants were harvested at 12 h postinfection (hpi). Infection with ME49 led to an ~7-fold induction of CCL2 secretion in BMDMs relative to uninfected BMDMs (Fig. 4A). This was reduced to, on average, ~4.5-fold in the GRA25-deficient parasites. This deficiency in CCL2 production was rescued in BMDMs infected with the complemented strain. Thus, consistent with our initial mapping data, CCL2 secretion levels are influenced by GRA25. Interestingly, the secretion of one other cytokine, CXCL1, was also significantly depressed in BMDMs infected with ME49Δ*gra25* parasites relative to ME49-infected macrophages ($P < 0.05$) and rescued in BMDMs infected with the complemented strain (Fig. 4A).

Since CCL2 is a key player in the immune response to *Toxoplasma* infection and mice deficient in CCL2 are more susceptible to *Toxoplasma* infection (8), we tested whether GRA25 is important for parasite virulence. Mice were infected by intraperitoneal injection with 500 tachyzoites of ME49, ME49Δ*gra25*, or ME49Δ*gra25*: GRA25$_{II}$ parasites and then monitored for weight loss and morbidity. All mice infected with the wild-type ME49 parasites died after 14 days; however, all mice infected with ME49Δ*gra25* parasites survived for the duration of the experiment (~2 months; Fig. 4B), a difference confirmed in 5 independent experiments. Importantly, parasite virulence was restored in the ME49Δ*gra25*: GRA25$_{II}$ complemented strain (Fig. 4B). Although they were avirulent, GRA25-deficient parasites were able to form cysts in the brains of chronically infected mice (data not shown), suggesting that the defect is likely in interaction with the immune system rather than in basic parasite biology. Cumulatively, these findings indicate that GRA25 is a novel parasite virulence factor.

Comparing the type II and type III alleles of GRA25. Based on data in ToxoDB, RNA expression levels for the *GRA25* gene do not appear to differ significantly between type II and type III strains. To investigate whether the protein levels for GRA25 differ between these two types, levels of endogenous GRA25 protein expression in type II (ME49-*luc*Δ*hxgprt*) and type III (CEPΔ*hxgprt*) parasites were compared by Western blot analysis. Lysates from equivalent numbers of type II and type III parasites were loaded, and membranes were probed using antisera generated against the type II version of GRA25. As expected, a band for GRA25 was observed in both type II and type III strains (Fig. 5A). Interestingly, however, there was more GRA25 signal in the type II lysates than in the type III lysates, and a loading control (antibody to the
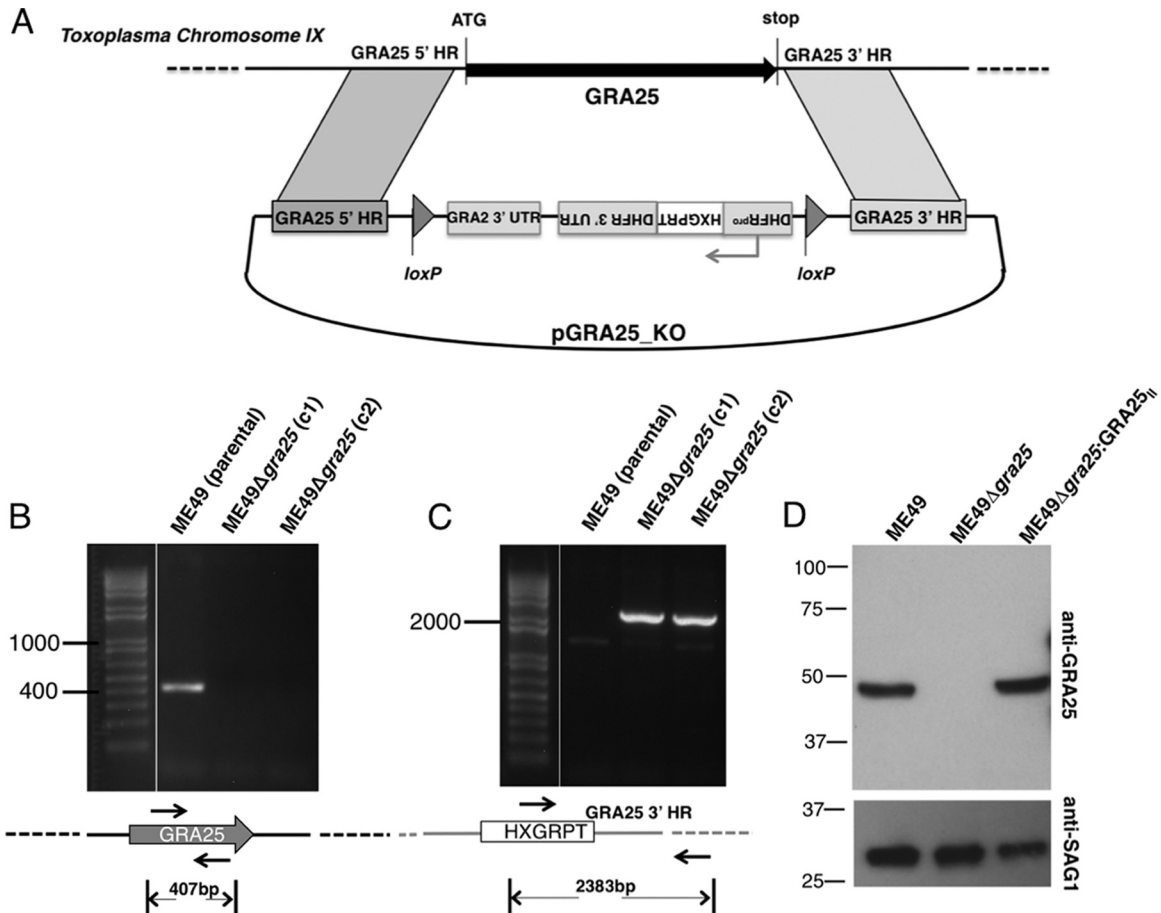
FIG 3 Generation and complementation of parasites deficient in *Toxoplasma* GRA25. (A) Schematic of the vector used for the double-crossover event to delete the *GRA25* coding region and replace it with an *HXGPRT*-selectable cassette driven by a *DHFR* promoter. Homology regions (HR) flanking the *GRA25* gene are shown. Bent arrows indicate promoters. *loxP* sites were used for Cre-mediated excision of the selectable marker in subsequent manipulations. The drawing is not to scale. UTR, untranslated region. (B) Verification of knockout by PCR. Primers were designed within the *GRA25* ORF to test for the presence of *GRA25* coding sequence in the type II parental strain, ME49, and in two independent ME49Δ*gra25* knockout clones, c1 and c2. All subsequent experiments were done with clone c1. (C) Primers in the *HXGPRT* sequence (forward) and in the region downstream of the *GRA25* 3′ HR used in the deletion construct (reverse) were used to confirm proper integration of the knockout cassette. The expected sizes of the amplification products are shown below the schematics. Relevant marker sizes (in bp) are shown on the left. The drawings are not to scale. (D) Parental (ME49), KO (ME49Δ*gra25*), or complemented (ME49Δ*gra25*:*GRA25*$_{II}$) parasite lysates were analyzed by SDS-PAGE. Membranes were probed with polyclonal anti-GRA25 mouse antisera and with anti-SAG1 antibodies (loading control). Migration of size markers is shown on the left (in kilodaltons). Experimental data are representative of the results of at least three independent experiments.

rhoptry neck protein, RON4) was used to confirm that equal amounts of parasite lysate were loaded in all lanes. To determine if the difference in anti-GRA25 signal was due simply to a reduced ability of the GRA25 antibody (which was raised against type II protein) to recognize the type III version, complemented parasites were generated in which an HA-tagged version of the type III allele of GRA25 was introduced into ME49Δ*gra25* (KO) parasites, resulting in ME49Δ*gra25*:*GRA25*$_{III}$ parasites. Lysates from these and ME49Δ*gra25*:*GRA25*$_{II}$ parasites were probed with anti-GRA25$_{II}$ antisera (Fig. 5B) and anti-HA antibodies (data not shown). The results showed comparable reactivities for the two antibodies, indicating that the two forms, at least when expressed in type II parasites, are equally capable of binding the polyclonal anti-GRA25 antibody. Thus, the difference seen in native lysates of type II and III parasites likely reflects a difference in the protein levels of GRA25 in these two strains. Given the similarities in RNA levels, this suggests differences in the stability and/or processing of

GRA25 in the two types. Importantly, in further characterization of endogenous GRA25 in the type II and type III strains, we observed that both type II GRA25 and type III GRA25 were secreted into the PV and showed similar localization results by IFA (data not shown).

Western blot analysis also revealed that the GRA25 band in type II parasites migrates more slowly than the band in type III parasites (Fig. 5A), even when the two allelic forms are expressed in the same (type II) genetic background (Fig. 5B). Since the two proteins are predicted to be about the same size (32.1 kb versus 32.2 for the type II and III versions, respectively) and pI (9.6 and 9.7, respectively), the mobility difference is surprising. While it could be due to differences in posttranslational modifications, such as phosphorylation, the serines and threonines in GRA25 that are known to be phosphorylated do not differ between the two allelic forms and the mobility difference was seen even when the genes were expressed in the same genetic background, arguing
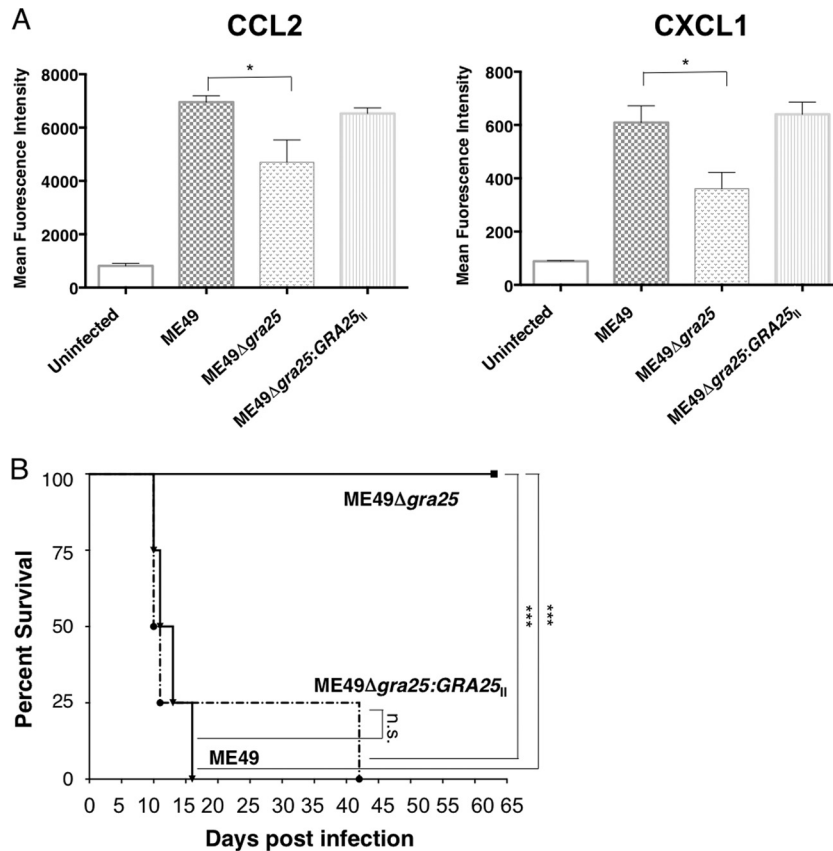
FIG 4 *Toxoplasma* GRA25 modulates cytokine secretion and is a novel parasite virulence factor. (A) Bone marrow-derived macrophages were infected with parental (ME49), KO (ME49Δ*gra25*), or complemented (ME49Δ*gra25*:*GRA25*$_{II}$) parasites at an MOI of 3. Cell culture supernatants were harvested at 12 hpi and passed through a 0.2-μm-pore-size filter, and mean fluorescence intensity (MFI) was determined for CCL2 and CXCL1 by Luminex mouse 26plex analysis. Data represent 3 independent experiments done on different days. Significance (*P*) was determined by a Mann-Whitney test. *, *P* < 0.05. (B) Female CBA/J mice were infected i.p. with 500 parental (ME49), KO (ME49Δ*gra25*), or complemented (ME49Δ*gra25*:GRA25$_{II}$) parasites. Survival was monitored each day postinfection. Significance (*P*) was determined by a log-rank (Mantel-Cox) test. ***, *P* < 0.007; n.s., not significant. Data are representative of the results determined for at least 20 mice per condition.

against these differences being due to strain-specific differences in protein kinases or other posttranslational modifiers. The molecular basis for this difference was not further pursued.

Given the differences we observed between type II and type III GRA25 proteins, we next sought to determine how expression of these alleles would affect the phenotype of the parasites expressing them *in vivo*. Mice were infected by intraperitoneal injection with 500 tachyzoites of ME49 (parental), ME49Δ*gra25* (KO), ME49Δ*gra25*:*GRA25*$_{II}$, or ME49Δ*gra25*:*GRA25*$_{III}$. Mice were monitored for weight loss and morbidity, and parasite growth was measured via bioluminescence imaging each day between 3 and 8 days postinfection (dpi) and at 10 dpi (by 11 dpi, some of the animals infected with the wild-type or complemented strains were exhibiting acute signs of the infection and had to be sacrificed). The results (Fig. 5C) showed that, while the ME49Δ*gra25* (KO) parasites (which are avirulent) initially grew as quickly as the wild-type ME49 (parental) parasites, starting at 4 or 6 dpi (depending on the experiment), their rate of expansion *in vivo* consistently slowed relative to that of ME49 parasites so that by 10 dpi, the level of parasite signal in the KO-infected mice was 20-fold lower than in wild-type-infected mice. This *in vivo* deficiency was fully rescued by complementation with both the type II and type III

GRA25 alleles (Fig. 5C). Consistent with these results, increased virulence was also restored to parasites complemented with the type III allele of GRA25 at the level seen in parasites complemented with the type II allele of GRA25 (see Fig. S2 in the supplemental material). Thus, GRA25 is a virulence factor that impacts the ability of the parasites to productively infect mice but the two allelic forms do not appear to confer levels of this *in vivo* phenotype that significantly differ, at least when expressed at similar levels and in the same (type II) genetic background.

DISCUSSION

The goal of this work was to identify important parasite effectors that influence the innate immune response to infection. Our results show that GRA25 is such a factor. GRA25 is crucial for parasite virulence and impacts CCL2 and CXCL1 production in infected macrophages. We have also found that while the type II and type III alleles of GRA25 are very different in sequence and differ in endogenous expression levels, both are able to promote parasite expansion *in vivo*. This result does not exclude the possibility that GRA25 contributes to virulence differences between type II and III, however, as the level of GRA25 expressed in the ME49Δ*gra25*: *GRA25*$_{III}$ strain was comparable to the levels seen in ME49Δ*gra25*:
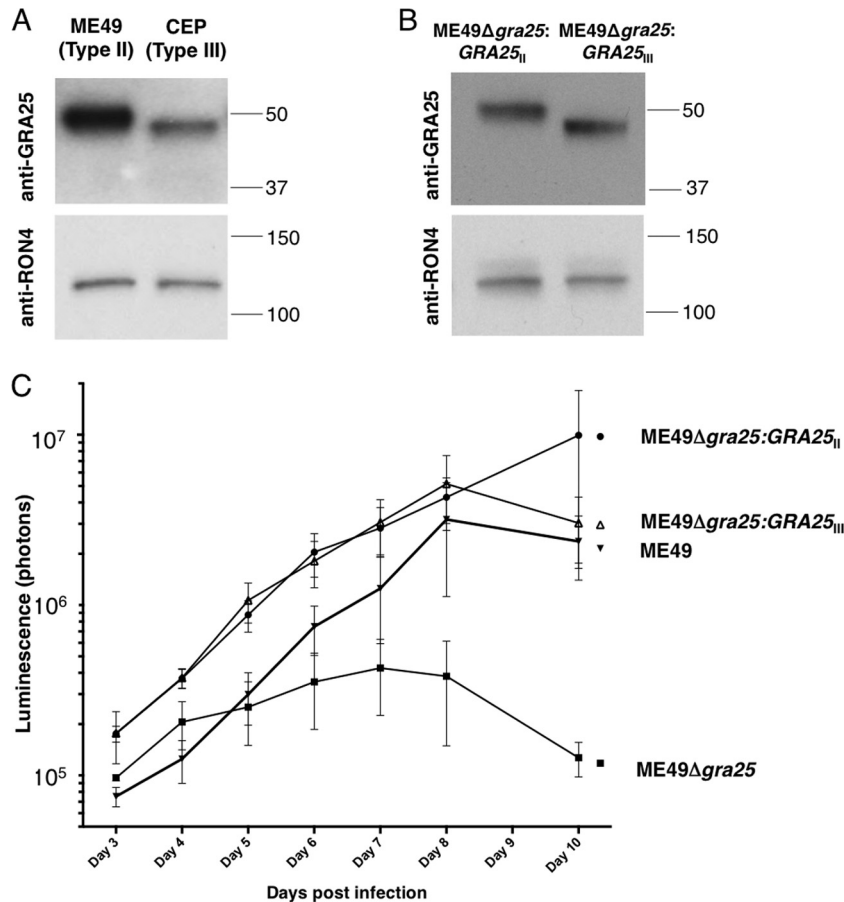
FIG 5 The type II and type III alleles of GRA25 differ in levels of endogenous expression and mobility; however, both promote parasite expansion *in vivo*. (A) Lysates of equivalent numbers of ME49 (type II) and CEP (type III) parasites were loaded in each lane. The membrane was probed using polyclonal antisera raised against GRA25 recombinant protein or RON4 (as a loading control). (B) Lysates of equivalent numbers of complemented type II (ME49Δ*gra25*:*GRA25*$_{II}$) or complemented type III (ME49Δ*gra25*:*GRA25*$_{III}$) parasites were loaded in each lane. The membrane was probed using polyclonal antisera raised against GRA25 recombinant protein or RON4 (as a loading control). (C) Female CBA/J mice were infected i.p. with 500 parental (ME49), KO (ME49Δ*gra25*), complemented type II (ME49Δ*gra25*:*GRA25*$_{II}$), or complemented type III (ME49Δ*gra25*:*GRA25*$_{III}$) parasites. Bioluminescence imaging was performed each day between 3 and 8 days postinfection (dpi) and at 10 dpi. Luminescence (photons) was quantified for the abdominal region for each mouse.

GRA25$_{II}$, whereas it is substantially lower in wild-type type III parasites. It may also be that GRA25 functions in association with other strain-specific parasite proteins and thus that expression of the type III allele in a type II background does not provide the protein with the strain-specific partners necessary to perform its endogenous function.

Despite multiple attempts, we were unable to obtain reliable data on the ability of the type III allele of GRA25 to rescue the decreased induction of CCL2 secretion by macrophages when infected with ME49Δ*gra25* parasites *in vitro*. We cannot comment, therefore, on whether GRA25 is responsible for the strain-specific effects on CCL2 expression, and we cannot exclude the possibility that another locus on chromosome IX also contributes to or is even solely responsible for that strain-specific difference. Nonetheless, the results presented here unequivocally demonstrate that *GRA25* is a key virulence gene in type II parasites and that it is necessary for the high levels of secretion of CCL2 seen in macrophages infected with this strain of parasites.

CXCL1 was also secreted at significantly lower levels in the ME49Δ*gra25*-infected cells than in cells infected with wild-type parasites. CCL2 and CXCL1 are both regulated by NF-κB, but so

too are several other cytokines whose expression was not significantly altered in the ME49Δ*gra25*-infected cells, and so the exact mechanism leading to the expression differences in just these two cytokines is not known. CXCL1 did not show a significant QTL peak for its expression in the analysis done on macrophages infected with the F1 progeny (data not shown), suggesting that either additional parasite factors beyond GRA25 affect its expression or, more likely, the strain-specific differences in GRA25 do not differentially impact its expression. The fact that both CCL2 and CXCL1 are regulated by NF-κB is likely to be the explanation for why removing GRA25 reduces the levels of their induction only partially: NF-κB levels are known to be modulated by several parasite-derived molecules, including glycophosphatidyl inositols (GPIs), profilin, GRA15, and GRA24 (13, 37–39). In our mapping of strain-specific *Toxoplasma* genes affecting CCL2 expression, we observed LOD score peaks on not only chromosome IX but also chromosome IV, suggesting that a gene on the latter chromosome may also be involved in CCL2 activation. Neither profilin nor GRA15 nor GRA24 is encoded on chromosome IV, but GPIs are the product of a complex biosynthetic pathway that has not been fully characterized in *Toxoplasma*. It is possible, therefore, that at

least one step in GPI biosynthesis is catalyzed by a protein encoded on chromosome IV and that this differs between types II and III. Alternatively, another parasite protein encoded on chromosome IV may be influencing the levels of NFκB and/or one of the other transcription factors that determines CCL2 levels in infected cells.

Cytokine secretion is critical for recruiting immune cells to clear *Toxoplasma* and for activating antiparasitic mechanisms within them, and so it was somewhat surprising to find that a strain that stimulates lower CCL2 levels (ME49Δ*gra25*) is less able to establish a productive infection in mice than wild-type ME49. This could be due to the fact that immune cells can also serve as a host cell in which *Toxoplasma* can grow, replicate, and disseminate. It is therefore possible that in the ME49Δ*gra25*-infected mice, reduced levels of cytokine lead to lower recruitment of target cells that *Toxoplasma* can infect and utilize as niches in which to replicate. While we have not determined whether there is a difference *in vivo* in the cytokine milieu or the cells recruited to the site of infection in mice infected with WT or Δ*gra25* parasites, it is known that CCL2, whose secretion is partly dependent on GRA25 *in vitro*, is critical for the recruitment of inflammatory monocytes during *Toxoplasma* infection (8).

Previous QTL mapping studies that identified *Toxoplasma* virulence factors used lethality in mice as the mapped phenotype. In those analyses, a small QTL peak was present on chromosome IX, but its association with strain-specific lethality in BALB/c and CD-1 mice was not statistically significant (40). This suggests that GRA25 is not a major strain-specific virulence factor, and our finding that the type II and type III alleles of this gene are equally able to rescue the attenuated phenotype of the ME49Δ*gra25* mutant is consistent with this conclusion. The work presented here nevertheless reveals that, as expected, virulence factors exist that are shared among strains. It also highlights the notion that studying a more subtle phenotype than lethality can lead to the identification of molecules that fine-tune the immune response and impact the course of infection in meaningful ways.

How GRA25 engages the infected host cell is not yet known, but we were able to visualize the protein on the bead-like "evacuole" structures that are sometimes seen emanating from the parasitophorous vacuole membrane (PVM) (data not shown) (25, 41). This could offer a clue to how GRA25 accesses the host cell and functions outside the parasitophorous vacuole. Alternatively, GRA25 proteins may use their putative transmembrane (TM) domain to integrate into the PVM and then be cleaved or further transported across the membrane as recently proposed for other GRA proteins (13, 37, 42). GRA25 lacks homology to any known parasite or eukaryotic proteins, but it is not unprecedented for a virulence factor to lack catalytic activity; in *Toxoplasma*, the most potent virulence factor discovered to date, ROP5, is comprised of a family of pseudokinases which, through binding the IRG substrate of the active kinase ROP18, facilitate the inactivation of those IRGs. It could be that GRA25 functions through a similar, "noncatalytic" mechanism, whereby it acts together with other host and/or parasite proteins to engage the production of cytokines.

Interestingly, the GRA25 transcript is expressed in at least three life cycle stages of the parasite: sporozoites, tachyzoites, and bradyzoites (35, 43–45), and the protein has likewise been readily detected in the tachyzoite and sporozoite stages (44). We have not investigated the function of GRA25 in the bradyzoite or sporozoite stages, but we did observe that GRA25-deficient parasites are able to form cysts in the brains of chronically infected mice (data not shown). We have not investigated the relative numbers of cysts in WT versus GRA25-deficient parasites because we used high doses in our infections to detect differences in virulence between the WT and Δ*gra25* strains. At these doses, WT mice succumbed to infection 10 to 14 dpi, before cysts could form. While we cannot exclude the possibility that GRA25 has distinct roles in different stages of the parasite, it is likely that this protein has a conserved, important role in infection across the three stages. Future studies using a nonlethal parasite dose will help to elucidate the effects of GRA25 on the immune response to *Toxoplasma* as well as the ability of the parasite to expand and persist in the host.

ACKNOWLEDGMENTS

REFERENCES

1. **Gazzinelli RT, Wysocka M, Hayashi S, Denkers EY, Hieny S, Caspar P, Trinchieri G, Sher A.** 1994. Parasite-induced IL-12 stimulates early IFN-gamma synthesis and resistance during acute infection with Toxoplasma gondii. J. Immunol. **153**:2533–2543.
2. **Denkers EY, Gazzinelli RT.** 1998. Regulation and function of T-cell-mediated immunity during Toxoplasma gondii infection. Clin. Microbiol. Rev. **11**:569–588.
3. **Denkers EY, Gazzinelli RT, Martin D, Sher A.** 1993. Emergence of NK1.1+ cells as effectors of IFN-gamma dependent immunity to Toxoplasma gondii in MHC class I-deficient mice. J. Exp. Med. **178**:1465–1472. http://dx.doi.org/10.1084/jem.178.5.1465.
4. **Scharton-Kersten TM, Wynn TA, Denkers EY, Bala S, Grunvald E, Hieny S, Gazzinelli RT, Sher A.** 1996. In the absence of endogenous IFN-gamma, mice develop unimpaired IL-12 responses to Toxoplasma gondii while failing to control acute infection. J. Immunol. **157**:4045–4054.
5. **Hunter CA, Sibley LD.** 2012. Modulation of innate immunity by Toxoplasma gondii virulence effectors. Nat. Rev. Microbiol. **10**:766–778. http://dx.doi.org/10.1038/nrmicro2858.
6. **Khaminets A, Hunn JP, Konen-Waisman S, Zhao YO, Preukschat D, Coers J, Boyle JP, Ong YC, Boothroyd JC, Reichmann G, Howard JC.** 2010. Coordinated loading of IRG resistance GTPases on to the Toxoplasma gondii parasitophorous vacuole. Cell. Microbiol. **12**:939–961. http://dx.doi.org/10.1111/j.1462-5822.2010.01443.x.
7. **Dunay IR, Damatta RA, Fux B, Presti R, Greco S, Colonna M, Sibley LD.** 2008. Gr1(+) inflammatory monocytes are required for mucosal resistance to the pathogen Toxoplasma gondii. Immunity **29**:306–317. http://dx.doi.org/10.1016/j.immuni.2008.05.019.
8. **Robben PM, LaRegina M, Kuziel WA, Sibley LD.** 2005. Recruitment of Gr-1+ monocytes is essential for control of acute toxoplasmosis. J. Exp. Med. **201**:1761–1769. http://dx.doi.org/10.1084/jem.20050054.
9. **Shi C, Pamer EG.** 2011. Monocyte recruitment during infection and inflammation. Nat. Rev. Immunol. **11**:762–774. http://dx.doi.org/10.1038/nri3070.
10. **Ong YC, Reese ML, Boothroyd JC.** 2010. Toxoplasma rhoptry protein 16 (ROP16) subverts host function by direct tyrosine phosphorylation of STAT6. J. Biol. Chem. **285**:28731–28740. http://dx.doi.org/10.1074/jbc.M110.112359.
11. **Saeij JP, Coller S, Boyle JP, Jerome ME, White MW, Boothroyd JC.** 2007. Toxoplasma co-opts host gene expression by injection of a polymorphic kinase homologue. Nature **445**:324–327. http://dx.doi.org/10.1038/nature05395.
12. **Yamamoto M, Standley DM, Takashima S, Saiga H, Okuyama M, Kayama H, Kubo E, Ito H, Takaura M, Matsuda T, Soldati-Favre D,**

Takeda K. 2009. A single polymorphic amino acid on Toxoplasma gondii kinase ROP16 determines the direct and strain-specific activation of Stat3. J. Exp. Med. **206:**2747–2760. http://dx.doi.org/10.1084/jem.20091703.

13. **Rosowski EE, Lu D, Julien L, Rodda L, Gaiser RA, Jensen KD, Saeij JP.** 2011. Strain-specific activation of the NF-kappaB pathway by GRA15, a novel Toxoplasma gondii dense granule protein. J. Exp. Med. **208:**195–212. http://dx.doi.org/10.1084/jem.20100717.

14. **Jensen KD, Hu K, Whitmarsh RJ, Hassan MA, Julien L, Lu D, Chen L, Hunter CA, Saeij JP.** 2013. Toxoplasma gondii rhoptry 16 kinase promotes host resistance to oral infection and intestinal inflammation only in the context of the dense granule protein GRA15. Infect. Immun. **81:**2156–2167. http://dx.doi.org/10.1128/IAI.01185-12.

15. **Fentress SJ, Behnke MS, Dunay IR, Mashayekhi M, Rommereim LM, Fox BA, Bzik DJ, Taylor GA, Turk BE, Lichti CF, Townsend RR, Qiu W, Hui R, Beatty WL, Sibley LD.** 2010. Phosphorylation of immunity-related GTPases by a Toxoplasma gondii-secreted kinase promotes macrophage survival and virulence. Cell Host Microbe **8:**484–495. http://dx.doi.org/10.1016/j.chom.2010.11.005.

16. **Fleckenstein MC, Reese ML, Konen-Waisman S, Boothroyd JC, Howard JC, Steinfeldt T.** 2012. A Toxoplasma gondii pseudokinase inhibits host IRG resistance proteins. PLoS Biol. **10:**e1001358. http://dx.doi.org/10.1371/journal.pbio.1001358.

17. **Niedelman W, Gold DA, Rosowski EE, Sprokholt JK, Lim D, Farid Arenas A, Melo MB, Spooner E, Yaffe MB, Saeij JP.** 2012. The rhoptry proteins ROP18 and ROP5 mediate Toxoplasma gondii evasion of the murine, but not the human, interferon-gamma response. PLoS Pathog. **8:**e1002784. http://dx.doi.org/10.1371/journal.ppat.1002784.

18. **Jensen KD, Wang Y, Wojno ED, Shastri AJ, Hu K, Cornel L, Boedec E, Ong YC, Chien YH, Hunter CA, Boothroyd JC, Saeij JP.** 2011. Toxoplasma polymorphic effectors determine macrophage polarization and intestinal inflammation. Cell Host Microbe **9:**472–483. http://dx.doi.org/10.1016/j.chom.2011.04.015.

19. **Pfefferkorn ER, Pfefferkorn LC, Colby ED.** 1977. Development of gametes and oocysts in cats fed cysts derived from cloned trophozoites of Toxoplasma gondii. J. Parasitol. **63:**158–159. http://dx.doi.org/10.2307/3280129.

20. **Pfefferkorn LC, Pfefferkorn ER.** 1980. Toxoplasma gondii: genetic recombination between drug resistant mutants. Exp. Parasitol. **50:**305–316. http://dx.doi.org/10.1016/0014-4894(80)90034-X.

21. **Caffaro CE, Koshy AA, Liu L, Zeiner GM, Hirschberg CB, Boothroyd JC.** 2013. A nucleotide sugar transporter involved in glycosylation of the Toxoplasma tissue cyst wall is required for efficient persistence of bradyzoites. PLoS Pathog. **9:**e1003331. http://dx.doi.org/10.1371/journal.ppat.1003331.

22. **Soldati D, Boothroyd JC.** 1993. Transient transfection and expression in the obligate intracellular parasite Toxoplasma gondii. Science **260:**349–352. http://dx.doi.org/10.1126/science.8469986.

23. **Coppens I, Dunn JD, Romano JD, Pypaert M, Zhang H, Boothroyd JC, Joiner KA.** 2006. Toxoplasma gondii sequesters lysosomes from mammalian hosts in the vacuolar space. Cell **125:**261–274. http://dx.doi.org/10.1016/j.cell.2006.01.056.

24. **Brymora A, Valova VA, Robinson PJ.** 2004. Protein-protein interactions identified by pull-down experiments and mass spectrometry. Curr. Protoc. Cell Biol. **22:**17.5.1–17.5.51. http://dx.doi.org/10.1002/0471143030.cb1705s22.

25. **Dunn JD, Ravindran S, Kim SK, Boothroyd JC.** 2008. The Toxoplasma gondii dense granule protein GRA7 is phosphorylated upon invasion and forms an unexpected association with the rhoptry proteins ROP2 and ROP4. Infect. Immun. **76:**5853–5861. http://dx.doi.org/10.1128/IAI.01667-07.

26. **Ong YC, Boyle JP, Boothroyd JC.** 2011. Strain-dependent host transcriptional responses to toxoplasma infection are largely conserved in mammalian and avian hosts. PLoS One **6:**e26369. http://dx.doi.org/10.1371/journal.pone.0026369.

27. **Subramanian A, Tamayo P, Mootha VK, Mukherjee S, Ebert BL, Gillette MA, Paulovich A, Pomeroy SL, Golub TR, Lander ES, Mesirov JP.** 2005. Gene set enrichment analysis: a knowledge-based approach for interpreting genome-wide expression profiles. Proc. Natl. Acad. Sci. U. S. A. **102:**15545–15550. http://dx.doi.org/10.1073/pnas.0506580102.

28. **Butcher BA, Fox BA, Rommereim LM, Kim SG, Maurer KJ, Yarovinsky F, Herbert DR, Bzik DJ, Denkers EY.** 2011. Toxoplasma gondii rhoptry kinase ROP16 activates STAT3 and STAT6 resulting in cytokine inhibition and arginase-1-dependent growth control. PLoS Pathog. **7:**e1002236. http://dx.doi.org/10.1371/journal.ppat.1002236.

29. **Brenier-Pinchart MP, Blanc-Gonnet E, Marche PN, Berger F, Durand F, Ambroise-Thomas P, Pelloux H.** 2004. Infection of human astrocytes and glioblastoma cells with Toxoplasma gondii: monocyte chemotactic protein-1 secretion and chemokine expression in vitro. Acta Neuropathol. **107:**245–249. http://dx.doi.org/10.1007/s00401-003-0804-0.

30. **Brenier-Pinchart MP, Pelloux H, Simon J, Ricard J, Bosson JL, Ambroise-Thomas P.** 2000. Toxoplasma gondii induces the secretion of monocyte chemotactic protein-1 in human fibroblasts, in vitro. Mol. Cell. Biochem. **209:**79–87. http://dx.doi.org/10.1023/A:1007075701551.

31. **Del Rio L, Butcher BA, Bennouna S, Hieny S, Sher A, Denkers EY.** 2004. Toxoplasma gondii triggers myeloid differentiation factor 88-dependent IL-12 and chemokine ligand 2 (monocyte chemoattractant protein 1) responses using distinct parasite molecules and host receptors. J. Immunol. **172:**6954–6960.

32. **Kim JM, Oh YK, Kim YJ, Cho SJ, Ahn MH, Cho YJ.** 2001. Nuclear factor-kappa B plays a major role in the regulation of chemokine expression of HeLa cells in response to Toxoplasma gondii infection. Parasitol. Res. **87:**758–763. http://dx.doi.org/10.1007/s004360100447.

33. **Hill RD, Gouffon JS, Saxton AM, Su C.** 2012. Differential gene expression in mice infected with distinct Toxoplasma strains. Infect. Immun. **80:**968–974. http://dx.doi.org/10.1128/IAI.05421-11.

34. **Minot S, Melo MB, Li F, Lu D, Niedelman W, Levine SS, Saeij JP.** 2012. Admixture and recombination among Toxoplasma gondii lineages explain global genome diversity. Proc. Natl. Acad. Sci. U. S. A. **109:**13458–13463. http://dx.doi.org/10.1073/pnas.1117047109.

35. **Treeck M, Sanders JL, Elias JE, Boothroyd JC.** 2011. The phosphoproteomes of Plasmodium falciparum and Toxoplasma gondii reveal unusual adaptations within and beyond the parasites' boundaries. Cell Host Microbe **10:**410–419. http://dx.doi.org/10.1016/j.chom.2011.09.004.

36. **Kim L, Butcher BA, Lee CW, Uematsu S, Akira S, Denkers EY.** 2006. Toxoplasma gondii genotype determines MyD88-dependent signaling in infected macrophages. J. Immunol. **177:**2584–2591.

37. **Braun L, Brenier-Pinchart MP, Yogavel M, Curt-Varesano A, Curt-Bertini RL, Hussain T, Kieffer-Jaquinod S, Coute Y, Pelloux H, Tardieux I, Sharma A, Belrhali H, Bougdour A, Hakimi MA.** 16 September 2013. A Toxoplasma dense granule protein, GRA24, modulates the early immune response to infection by promoting a direct and sustained host p38 MAPK activation. J. Exp. Med. http://dx.doi.org/10.1084/jem.20130103.

38. **Debierre-Grockiego F, Campos MA, Azzouz N, Schmidt J, Bieker U, Resende MG, Mansur DS, Weingart R, Schmidt RR, Golenbock DT, Gazzinelli RT, Schwarz RT.** 2007. Activation of TLR2 and TLR4 by glycosylphosphatidylinositols derived from Toxoplasma gondii. J. Immunol. **179:**1129–1137.

39. **Yarovinsky F, Zhang D, Andersen JF, Bannenberg GL, Serhan CN, Hayden MS, Hieny S, Sutterwala FS, Flavell RA, Ghosh S, Sher A.** 2005. TLR11 activation of dendritic cells by a protozoan profilin-like protein. Science **308:**1626–1629. http://dx.doi.org/10.1126/science.1109893.

40. **Saeij JP, Boyle JP, Coller S, Taylor S, Sibley LD, Brooke-Powell ET, Ajioka JW, Boothroyd JC.** 2006. Polymorphic secreted kinases are key virulence factors in toxoplasmosis. Science **314:**1780–1783. http://dx.doi.org/10.1126/science.1133690.

41. **Håkansson S, Charron AJ, Sibley LD.** 2001. Toxoplasma evacuoles: a two-step process of secretion and fusion forms the parasitophorous vacuole. EMBO J. **20:**3132–3144. http://dx.doi.org/10.1093/emboj/20.12.3132.

42. **Bougdour A, Durandau E, Brenier-Pinchart MP, Ortet P, Barakat M, Kieffer S, Curt-Varesano A, Curt-Bertini RL, Bastien O, Coute Y, Pelloux H, Hakimi MA.** 2013. Host cell subversion by Toxoplasma GRA16, an exported dense granule protein that targets the host cell nucleus and alters gene expression. Cell Host Microbe **13:**489–500. http://dx.doi.org/10.1016/j.chom.2013.03.002.

43. **Buchholz KR, Fritz HM, Chen X, Durbin-Johnson B, Rocke DM, Ferguson DJ, Conrad PA, Boothroyd JC.** 21 October 2011. Identification of tissue cyst wall components by transcriptome analysis of in vivo and in vitro Toxoplasma bradyzoites. Eukaryot. Cell http://dx.doi.org/10.1128/EC.05182-11.

44. **Fritz HM, Bowyer PW, Bogyo M, Conrad PA, Boothroyd JC.** 2012. Proteomic analysis of fractionated Toxoplasma oocysts reveals clues to their environmental resistance. PLoS One **7:**e29955. http://dx.doi.org/10.1371/journal.pone.0029955.

45. **Fritz HM, Buchholz KR, Chen X, Durbin-Johnson B, Rocke DM, Conrad PA, Boothroyd JC.** 2012. Transcriptomic analysis of toxoplasma development reveals many novel functions and structures specific to sporozoites and oocysts. PLoS One **7:**e29998. http://dx.doi.org/10.1371/journal.pone.0029998.